SPOT WELDING RESIDUAL STRESSES ASSESSMENT USING NONLINEAR NUMERICAL TECHNIQUE

Dr. Nabeel K. Alsahib
University of Baghdad
AL-Khwarizmi college of Eng.

Dr. Somer M. Nacy
University of Baghdad
AL-Khwarizmi college of Eng.

Dr. Faiz F. Mustafa
University of Baghdad
AL-Khwarizmi college of Eng

ABSTRACT

A description is given of the resistance spot welding process in terms of internal behavior of the weld as welding takes place. Heat input due to spot welding of steel sheet plate causes temperature gradient in the parent metal. After cooling, residual stresses appear around the welding zone reducing the strength. Residual stresses are a result of the temperature gradient and the dependency of material properties on the temperature, such as yield strength, elasticity modulus, and thermal expansion coefficient. Nonlinear transient heat transfer analysis performed in order to obtain the temperature distribution in the welded part .A nonlinear thermo–plastic stress analysis is then performed to predict the stress and strain fields during and after welding. The material properties such as yield strength, elasticity modulus, convection coefficient, conduction, specific heat, and thermal expansion coefficient are used as a function of temperature. The heat transfer results are compared with experimental results performed within the scope of work of this study. On the other hand, the residual stress results are compared with experimental result obtained from literature .The comparison shows good agreement between numerical and experimental results.

الخلاصة:

يقدم البحث وصف دقيق لعملية اللحام النقطي على اساس التغيرات الداخليه الحاصله في المعدن أثناء وبعد عملية اللحام, حيث اعتمدت طريقة رقمية لاخطية معتمدة على العناصر المحددة يمكن من خلالها تعيين درجات الحرارة الناجمة عن عملية اللحام النقطي وتغييرها مع المسافة والزمن ((انتقال الحرارة اللاخطي والمعتمد على التغيير مع الزمن)) ومن ثم يمكن بأستخدام طريقة العناصر المحددة اللاخطية ((اللدونة الحرارية)) لتعيين الأجهادات المتبقية في الجزء الملحوم وما حوله بعد عملية التبريد. ان الاجهادات المتبقيه تظهر نتيجة لتغير درجات الحراره وما يصاحبها من تغير في خواص المعدن مثل مقاومة الخضوع, حد المرونه, معامل التمدد الحراري ومعامل التوصيل والحمل مع التغير في درجات الحرارة, ولقد تم اجراء تجارب لقياس درجات الحرارة للجزء الملحوم أثناء وبعد عملية اللحام في اجزاء وأزمنة مختلفة لمقارنتها بالنتائج الرقمية ، وتم الأعتماد على تجارب لقياس الأجهادات المتبقية أجريت في أبحاث أخرى للمقارنة حيث ظهر صلاحية الطرق الرقمية بكفاءة عالية وخاصة لتعيين درجات الحرارة وذلك نتيجة دقة التمثيل الرقمي في وصف وتغيرها مع الحرارة ووصف الظروف المحيطة سواء التمثيل الحراري أو الأجهادات.

KEYWORDS

Heat transfer, Residual stress, Finite element, Spot weld, Stainless steel.

INTRODUCTION

Residual stress distribution and distortion in welded plates are strongly affected by many parameters and by their interaction. In particular, there are structural, material and welding factors. The structural parameters include geometry of the plates, thickness and width and joint type. Among the material parameters mechanical and physical properties. Welding variables such as current, force, and weld time .As a consequence of the non-uniform temperature distribution, parts of material close to the weld is subjected to different rates of expansion and contraction developing a three-dimensional complex residual stress state, **(Sarkani and Lutes, 1988)**. To understand the formation of residual stress, node temperature history during the welding process must be calculated. During the weld thermal cycle material mechanical properties change–drastically, especially when material approaches melting temperature. Therefore, due to the temperature dependence of material properties and the large deformation in welding, material and geometrical non-linearity have to be taken into account .The initial expansion of material due to the temperature increase is constrained by material placed away form the heat source. Therefore generating compressive stress .At a temperature higher than material critical temperature, the material starts exhibiting thermal softening where heating results in decrease of flow stress .As phase change occurs deviatory stress become zero and considerable plastic deformation occurs in the weld metal and the base metal near the weld. As temperature decreases during the cooling phase, the stress in the solidifying martial increases, and become tensile due to the positive temperature gradient. The region placed away form the welding area, will therefore, be in compression since the resultant force and the resultant moment induced by residual stress evaluated in the center spot plane section must satisfy translation and rotational equilibrium. Plate stiffness affects strongly magnitude and distribution of residual stress. In some cases, residual stress may or exceed the yield stress of the parent plate material, **(Tall, 1964), (Sun and Dong, 2000).** The plastic strains resulting from heating induce stress, which in turn produce internal forces that may cause bending and rotation. The displacements are in general called distortion. The residual stress combined with distortion and degradation of the material mechanical properties influence the buckling strength and fatigue life of welded structure.

FINITE ELEMENT MODELING PROCEDURE

Spot welding is a material joining technology using electrical resistance heat of metallic and it is a complicated phenomena. The FE analysis was carried out in two steps (coupled-field analysis that coupling between two or more fields of engineering). A non-linear transient thermal analysis was conducted first to obtain the global temperature history generated during the welding process. A stress analysis was then developed with the temperatures obtained from the thermal analysis used as loading to the stress model, M. Meo and R. Vignjevic. In this analysis, the left and bottom edge of **Fig. 1,** are symmetry axes so only one quadrant of the weld nugget (upper right corner) is shown, ANSYS (8) package was used with an ax symmetric 2D model; solid 8-node element**.**

The accuracy of the FE method depends upon the density of the mesh used in the analysis. Both the stress and thermal analysis have identical meshes. The weld nuggets temperature is higher than the melting point of the material, and it drops sharply in regions away from the weld nugget. Therefore in order to obtain the correct temperature field in the region of high temperature gradients it was necessary to have a more refined mesh close to the weld nugget. While in regions located away from weld-nugget a more coarse mesh was used. Sensitivity

analysis of mesh density was performed and a satisfactory mesh was adopted for further studies, the higher is the heat input the higher is the number of nodes necessary to accurately interpolate high temperature gradient, H. Huh and Kang, 1997. A stainless steel (304) material property was used for FE model. The chemical composition, mechanical properties of the specimens at room temperature are given in **Table 1&2,** respectively, William, and spot welding condition described in **Table 3,** Roy and Norman, 1976.

NON-LINEAR TRANSIENT HEAT TRANSFER NUMERICAL MODEL

One of the fundamental problems in the analysis of heat flow during welding is how to take into account physical material changes due to temperature changes during the welding process. If the material properties are treated as temperature dependent the **eq. (1)** of heat –flow become non-linear, Cosmos, 2000.

$$\rho \frac{\partial c_p T}{\partial t} = Q + \frac{\partial (k \times \frac{\partial T}{\partial X})}{\partial X} + \frac{\partial (ky \frac{\partial T}{\partial y})}{\partial y} + \frac{\partial (k_z \frac{\partial T}{\partial Z})}{\partial Z} \quad (1)$$

Where cp is the specific heat, K thermal conductivity, T temperature, Q is the volumetric heat generation and t is time .If the material properties are considered temperature independent the equation (specific heat, thermal conductivity do not change with temperature) is reduced to a linear differential **eq. (2).**

$$\rho c_p \frac{\partial T}{\partial t} = Q + K(\frac{\partial (\frac{\partial T}{\partial X})}{\partial X} + \frac{\partial (\frac{\partial T}{\partial y})}{\partial y} + \frac{\partial (\frac{\partial T}{\partial Z})}{\partial Z}) \quad (2)$$

In the current analysis temperature-dependent thermal properties were assumed, therefore non-linear equations were obtained and solved. **Fig. 2,** shows the thermal specific heat (CP), conductivity (K=Kx=Ky=Kz), and convection coefficient relationship with temperature, Ajinomoto, 2001. The material density is approximately considered constant (7850 kg/m^3). To determine temperature and other thermal quantities that vary over time there was the need to perform a transient thermal analysis. Implicit method of time discrimination was employed which allows for larger time steps .It is important not to forget that time step size is not a problem with respect to calculation stability but it determines the accuracy of the solution. Using the FE analysis the thermal and stress analysis are uncoupled while in reality thermal effect and mechanical deformation occur at the same time .The de-coup line of the analysis becomes acceptable if one assumes that dimensional change (mechanical deformation) during welding process are negligible because thermal energy change is predominant over mechanical work done during welding, and the internal energy dissipation effect on the temperature distribution is negligible. Therefore to evaluate distortion and residual stress distribution the thermal analysis was performed first in order to find nodal temperature as a function of time. Once defined temperature history for each node, temperature loads were applied to the structural model. Temperature history can be shown in **Fig. 3.** The heat within a spot weld is generated totally by resistance to the high electric current passing through the joint and consequently the points of greatest heat generation are the points of greatest resistance (faying surface) .The plate absorbs a part of the heat generated. There are losses from the surfaces in the form of convection. Therefore, to evaluate the amount of heat absorbed by the plates as a portion of the total heat generated the following formula was used, **(Milner and Apps, 1968).**

$$Q = I^2 Rt \quad (3)$$

Where I is the welding current, R is the faying surface resistance and t the time of welding.

The assumptions made are:

- Thermal properties, i.e. conductivity, specific heat and convection are temperature dependent.
- Effects arising from phase change are taken in to account, enthalpy change during the phase change.
- Heat losses by transfer to the ambient medium by radiation are negligible.

Convection losses are evaluated using the **eq. (4)**

$$Q_i = hA_i(T_i - T_\circ) \tag{4}$$

Where h is the convection heat transfer coefficient (for free convection in air, h has maximum of $(9W/m^2 - C^\circ)$), **(Chapman, 1987)**. Q_i denotes the heat loss on surface i with area A_i , T_i is the temperature on surface A_i , and $T_\circ$ is the ambient temperature.

During the welding process phase change occurred, to account the effect of latent heat, i.e. heat energy which, is released or stored by the material during a phase change enthalpy was specified. The concept that could be readily adopted by the finite element was formulated on the basic of integrating the heat capacity of the material over a small region of phase changes (see **eq. (5)**), **(Tekriwal and Mazumunder, 1988)**.

$$H_{(T)} = \int \rho C_p(T)dT \tag{5}$$

EXPERIMENTAL RESULTS FOR HEAT TRANSFER PROBLEM

The experimental temperature of melting pool zone could not be measured with simple technique such as thermocouples, but in the region away from weld nugget, peak temperature was measured using a thermocouple located at five different positions A, B, C, D and E from the center of spot as shown in **Fig. 4.** The temperature measured from the experiment and the temperature result from the numerical analysis can be shown in **Fig. 5.** The nodal numerical results temperature distribution for the (0.6mm) plate at different time steps during welding and cooling are shown in the **Fig. 6,** and **Table 4,** gives the maximum temperature measured compared with temperature calculated and its discrepancy.

NON-LINEAR NUMERICAL MODEL FOR RESIDUAL STRESS

An important problem in the analysis of residual stress during welding is how stress develops in region near the welding nugget when structural members are joined by spot welding the material of the plates has to be heated to its melting point and then cooled again rapidly under restraint conditions imposed by the geometry of the joint. As a result of this severe thermal cycle the original microstructure and properties of the metal in a region close to the weld are change. This part of the metal, or zone, is usually referred to as heat–affected zone (HAZ). The change in the HAZ dependent upon the thermal and mechanical history of the metal. Therefore, after the welding

process there will be different zones with different mechanical properties. In particular, there is a softening of the material in the HAZ, and decrease mechanical properties, i.e. Yield strength, ultimate strength, but elastic modulus remains unaffected by the welding process, **(Mansubuchi, 1980)**.

After calculation the temperature distribution in time, the next step was to find distortion and residual stress distribution. The residual stress distribution calculation was based on the following assumptions:

- Parent plate metal and welded zone metal have the same mechanical properties, i.e. softening of material was neglected.
- Deformation process was rate independent, and a elastic – plastic constitutive model with isotropic hardening was assumed for the material.
- Mechanical properties depend on temperature as shown in **Fig. 7.**

The analysis was performed for the time period between the start of welding and the end of cooling phase. Within each time increment, the solution of elastic–plastic problem was found by linearzing the non-linear stress–strain curved. The analysis was performed and stresses and displacements were calculated by Newton–Raphson iterative process. The iterations were repeated until convergence is achieved. Boundary conditions were imposed to prevent any rigid body motion of the plate. Additional symmetry boundary conditions were imposed since only half of the plate was analyses.

RESULTS AND DISCUSSIONS

It is found that magnitude and distribution of residual stress is strongly affected by:

- Temperature gradient and distribution through the thickness and width of the plates.
- Thermal expansion coefficients of the materials.
- Mechanical properties of material at elevated temperature

The longitudinal residual stress distribution is shown in **Fig. 8,** evaluated at middle cross-section, bottom surface of spot. The positive stress (tension) in x direction peak of (317 MPa) is at the weld area, while away from the weld center the stress is negative (compression) and the maximum is (21 MPa). The shape of longitudinal stress distribution dose not change but the stress amplitude decreases towards the top surface when the maximum longitudinal stress is (91 MPa) seeing **Fig. 9, 10.** This was due to the assumption that heat generation was coming through the bottom weld surface. The Von Misses stress distribution over the entire plate is shown in **Fig. 11.** The peak stress is (321 MPa) close to the material yield strength. The out-of-plane displacement is shown in **Fig. 12,** and the maximum displacement amplitude was 0.0074mm, this means that the out-of-plane displacement was 1.23% of plate thickness. The displacement is very important for the buckling behavior of welded panel. The other displacement UX, (see **Fig. 13**) are negligible compared to the UY. For a similar plate with same geometry, same boundary condition with higher thickness, residual stress would be higher but distribution would become smaller due to the increased in stiffness of the plate, Meo and Vignjevic. The residual stress results are verified with experimental measurements obtained from literature, where the longitudinal stress reach a maximum of (301 MPa) in tension and (17 MPa) in compression. Such a discrepancy between the numerical and experimental values for welding residual stress may be attributed to the difference between the condition of the numerical analysis and the experiment. The nugget metal was actually pressed out by the electrode force and thermal expansion. However, such actual welding condition and various thermal and physical properties were neglected in the process of the FEA. Also, the releases of residual stress when cutting off the plate with wet machining were not considered in the FE analysis.

CONCLUSION

The residual stress and distortion for the 304 stainless steel plate were calculated. De–coupled thermal and structural analyses were performed. Good correlation between experimental results and analytical calculation was achieved. In particular, an error of 6.12% between calculated temperature profile and experimental measurement was found. Residual stress distribution agrees with the experimental result obtained with an error of 5% for the tension–stress and 19% for the compression.

REFERENCES

Ajinomoto .T Bldg "Nippon Yakin Kogyo co." Material Property Data.

Chapman, A. J., "Fundamentals of Heat Transfer", Macmillan, New York. 1987.

Cosmos / M finite Element Software, Advanced Modules Theoretical Manual SRAC, Los Angeles, California, USA, 2000.

D.R. Milner and R.L. Apps "Introduction to Welding and Brazing" Library of Congress Catalog. 1968.

Faiz F. Mustafa, "Static and Dynamic Analysis of Plates with Spot Welded Stiffeners", Ph.D. thesis, University of Baghdad, College of Engineering, Mech. Dept., October 2006.

H. Huh and W.J Kang "Electro thermal Analysis of Electric Resistance Spot Welding processes by a 3-D finite Element Method" Journal of Materials processing Technology, 63, PP. 672-677, 1997.

Mansubuchi K. "Analysis of welded structure". Pergaman Press. Oxford , 1980.
M. Meo and R.Vignjevic "welding Simulation Using FEA" College of Aeronautics, Canfield University, Bedford, UK, MK43 OAL.

Roy. A. Linderg and Norman R. Braton "welding and other Joining Processes 1976.

Sarkani, S.S. and Lutes, L.D., "Residual Stress Effect in Fatigue of Welded Joints", Journal of Structural Engineering, Vol, 114 No.2, PP. 462-474, Feb.1988.

Tall L., "Recent Developments in the Study of Column Behaviour". Four. Inst. Engrs., pp. 319-333, Aust., Dec. 1964.

Tekriwal P., Mazumunder J., "Finite Element Analysis of Three Dimensional Transient Heat Transfer in GMA", Welding Journal, 1988.

William H. Cubberly," Metals Handbook "Ninth Edition, American Society for Metals.

X.Sun and P.Dong, "Analysis of Aluminum Resistance Spot welding Processes using Coupled finite Element Procedures", Welding research supplement, PP. 215s-221s, August, 2000.

SYMBOLS

A Area (mm^2)

Cp Specific heat $(w.\sec/kg.c^\circ)$

H Enthalpy $(w.\sec.c^\circ/mm^3)$

h Convection heat transfer $(w/mm^2.c^\circ)$

I Welding current (Amp)
K Thermal conduction ($w/mm.c^{\circ}$)
Q Heat generation ($w.\sec/mm^3$)
Qi Heat losses ($w.\sec$)
R Surface resistance
T Temperature (c°)
t Time (sec)

Table 1 - Chemical composition of stainless steel (304**)**, William.

	C	Cr	Fe	Mn	N	Ni	P	S	Si
Stainless steel (304)	**0.08**	**18-20**	**71**	**2**	**0.1**	**8-11**	**0.045**	**0.03**	**1**

Table 2 – Mechanical properties of stainless steel (304), William.

	Tensile strength (MPa)	Yield strength (MPa)	Modulus of Elasticity (GPa)	Elongation %
Stainless steel (304)	**572**	**290**	**200**	**50**

Table 3 – Welding condition of stainless steel (304), Roy and Norman.

	Electrode force (N)	Welding current (A)	Welding time (cycles)	Tip diameter (mm)
Welding condition	**2300**	**4000**	**12**	**0.5**

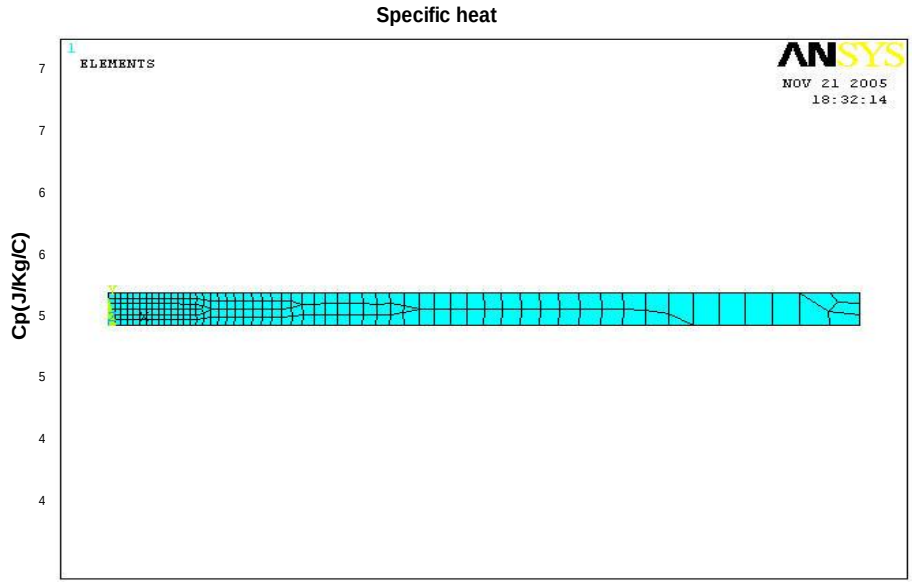

Fig. 1. Finite Element Model and Mesh

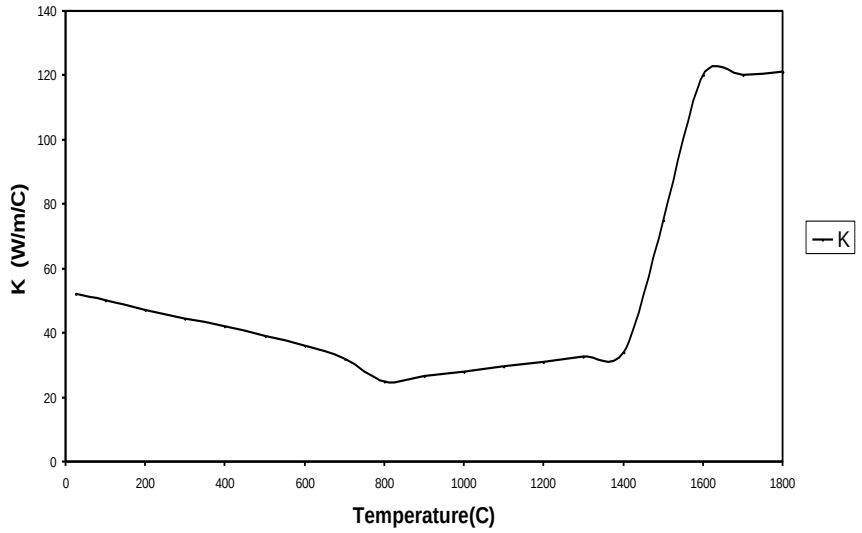

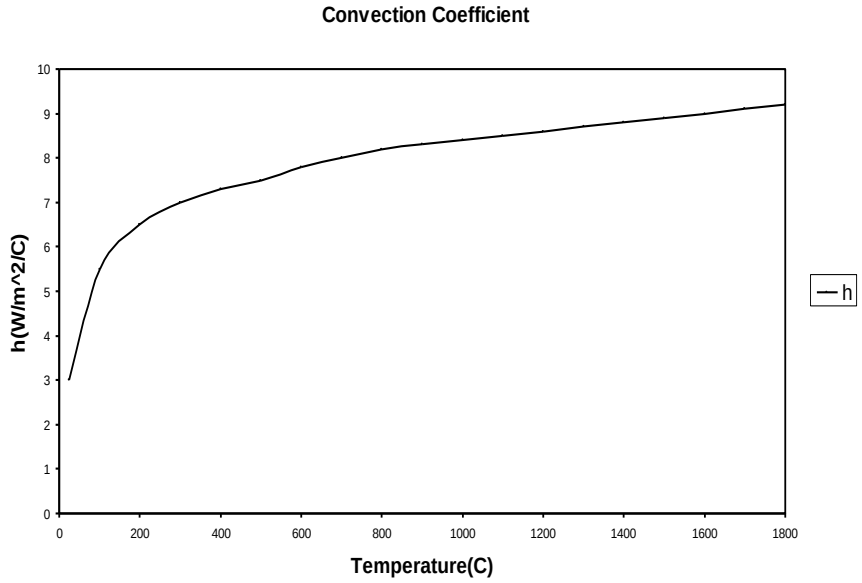

Fig. 2. Variation of Heat Transfer Parameters with temperature, Ajinomoto, 2001

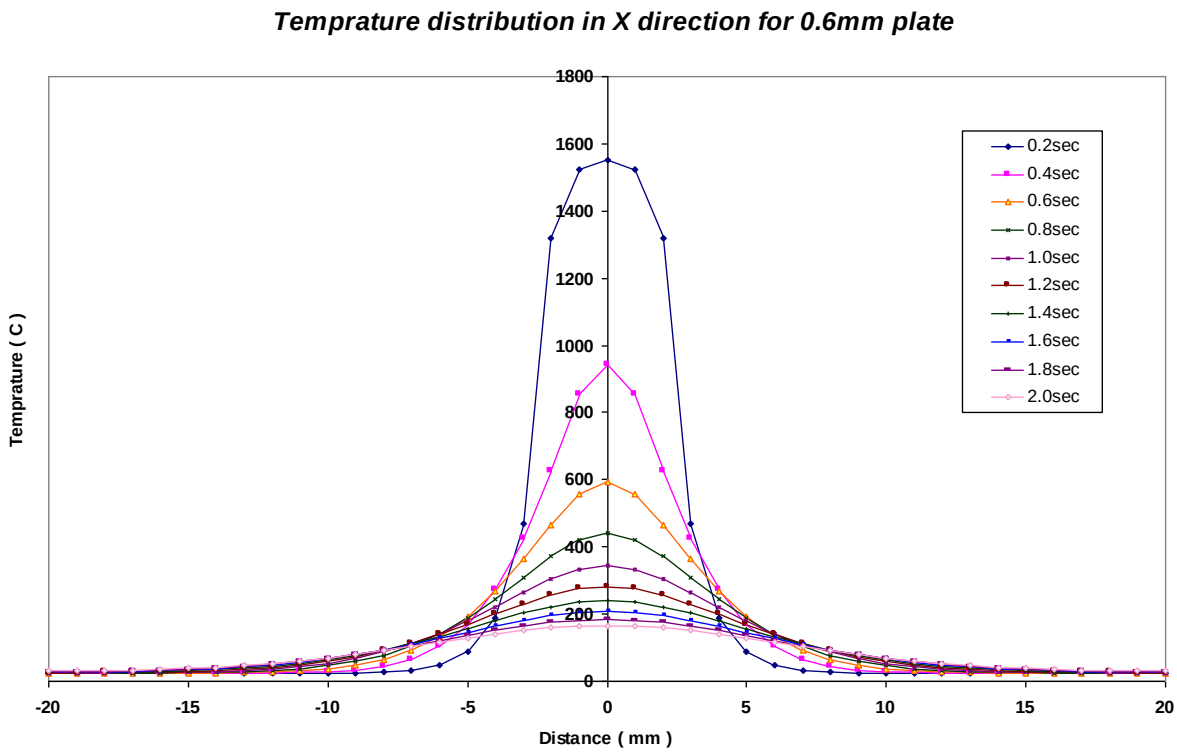

Fig. 3. Temperature distribution in X direction for 0.6mm plate

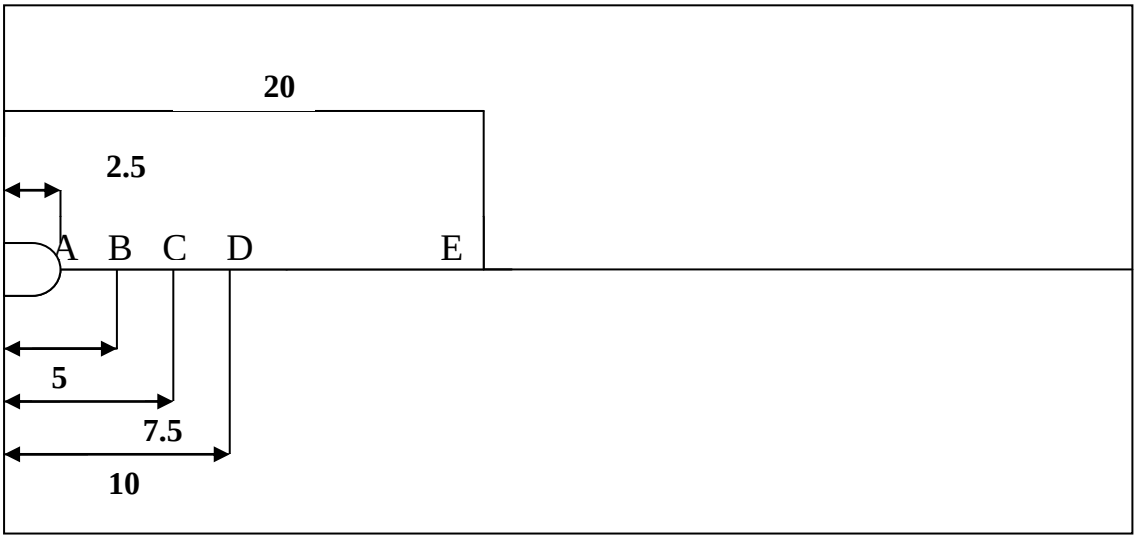

Fig. 4. Holes Positions of Thermocouples (mm).

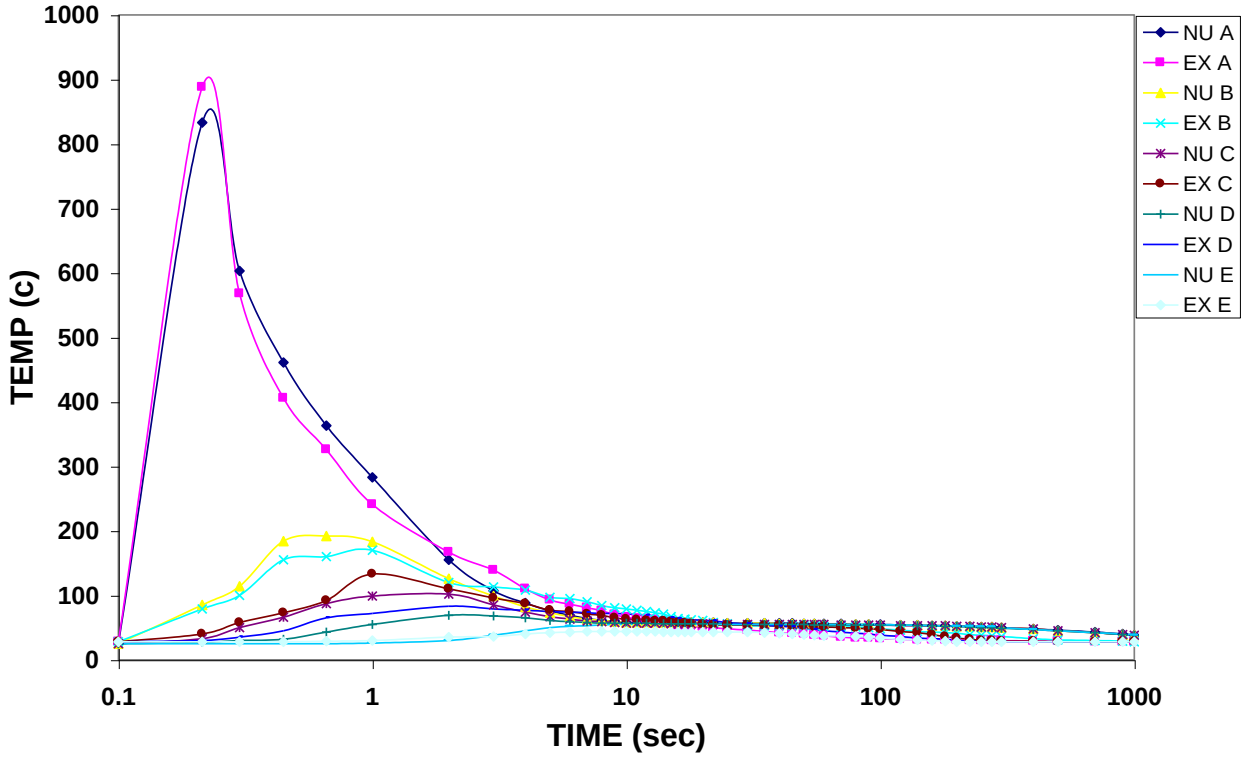

Fig. 5. Computed and measured temperature for 0.6mm plate

Table 4 - Maximum Numerical and Experimental Temperature.

Measured Point	Maximum Numerical Temperature	Maximum Experimental Temperature	Discrepancy %
A	833	888	+6.2
B	192	179	-7.2
C	102	112	+8.9
D	73	79	+7.6
E	55	51	-7.8

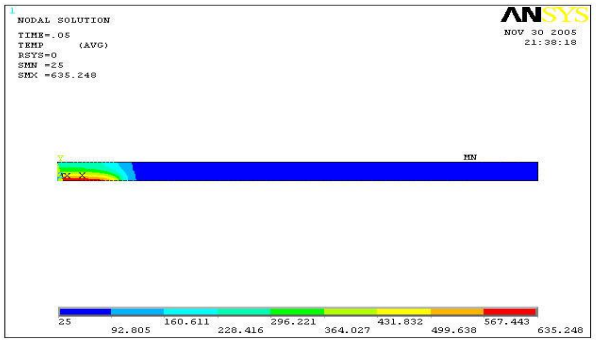

a. Time = 0.05 sec

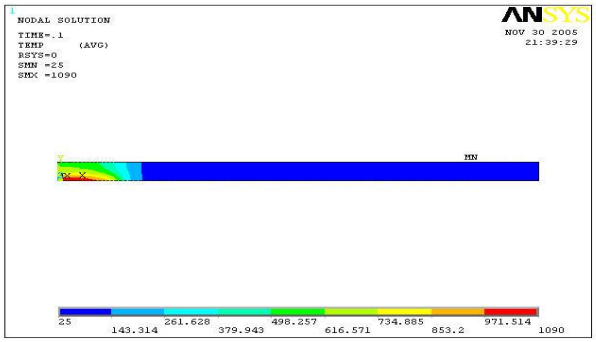

b. Time =0.1sec

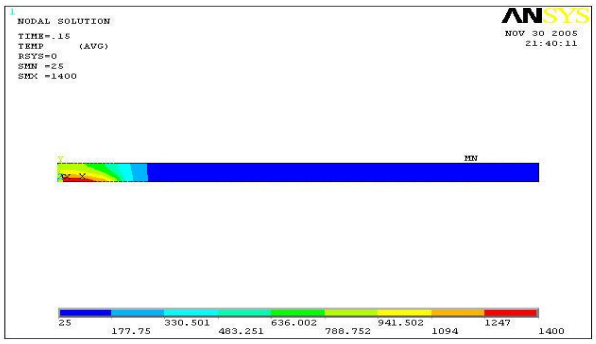

c. Time =0.15 sec

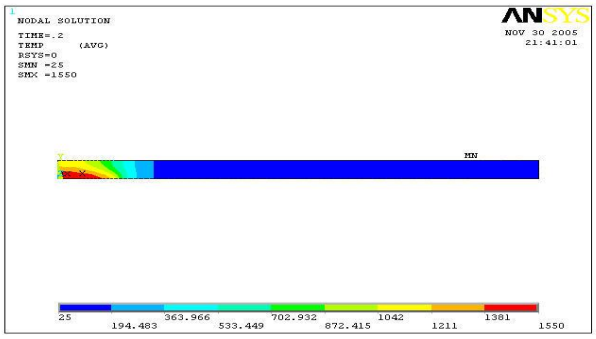

d. Time = 0.2 sec

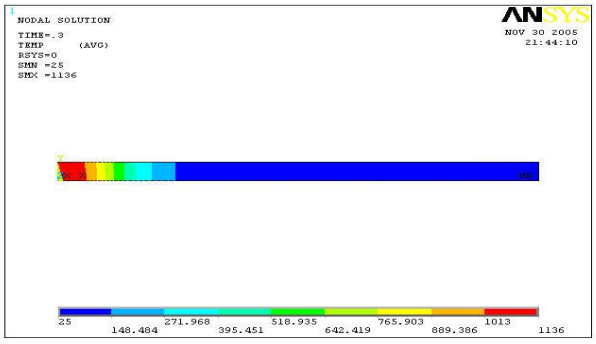

e. Time = 0.3 sec

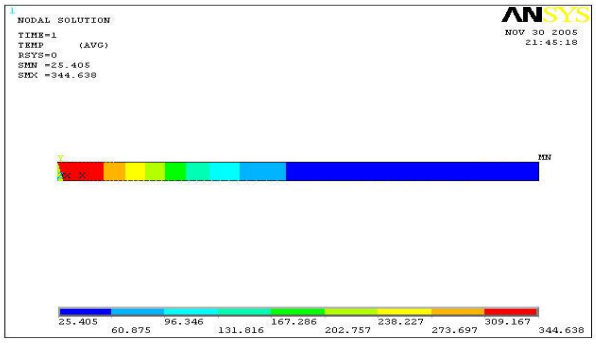

f. Time = 1sec

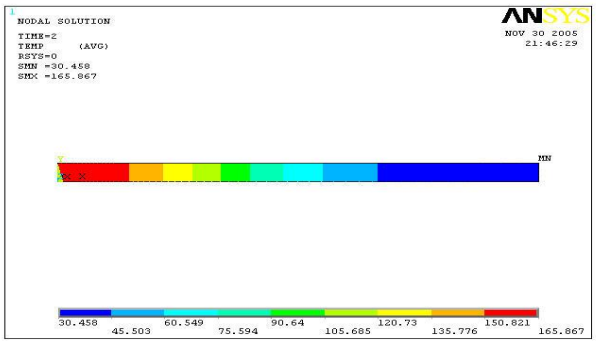

g. Time = 2sec

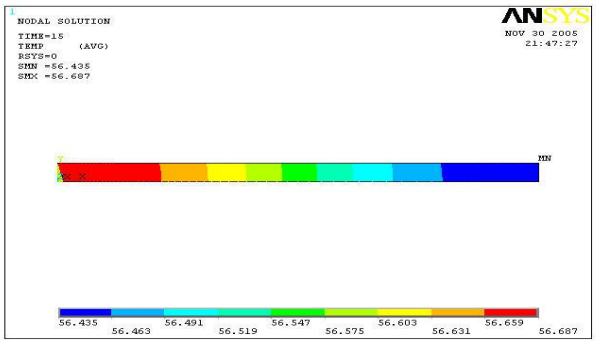

h. Time = 15sec

Fig. 6. Temperature distribution at different time for 0.6mm plate

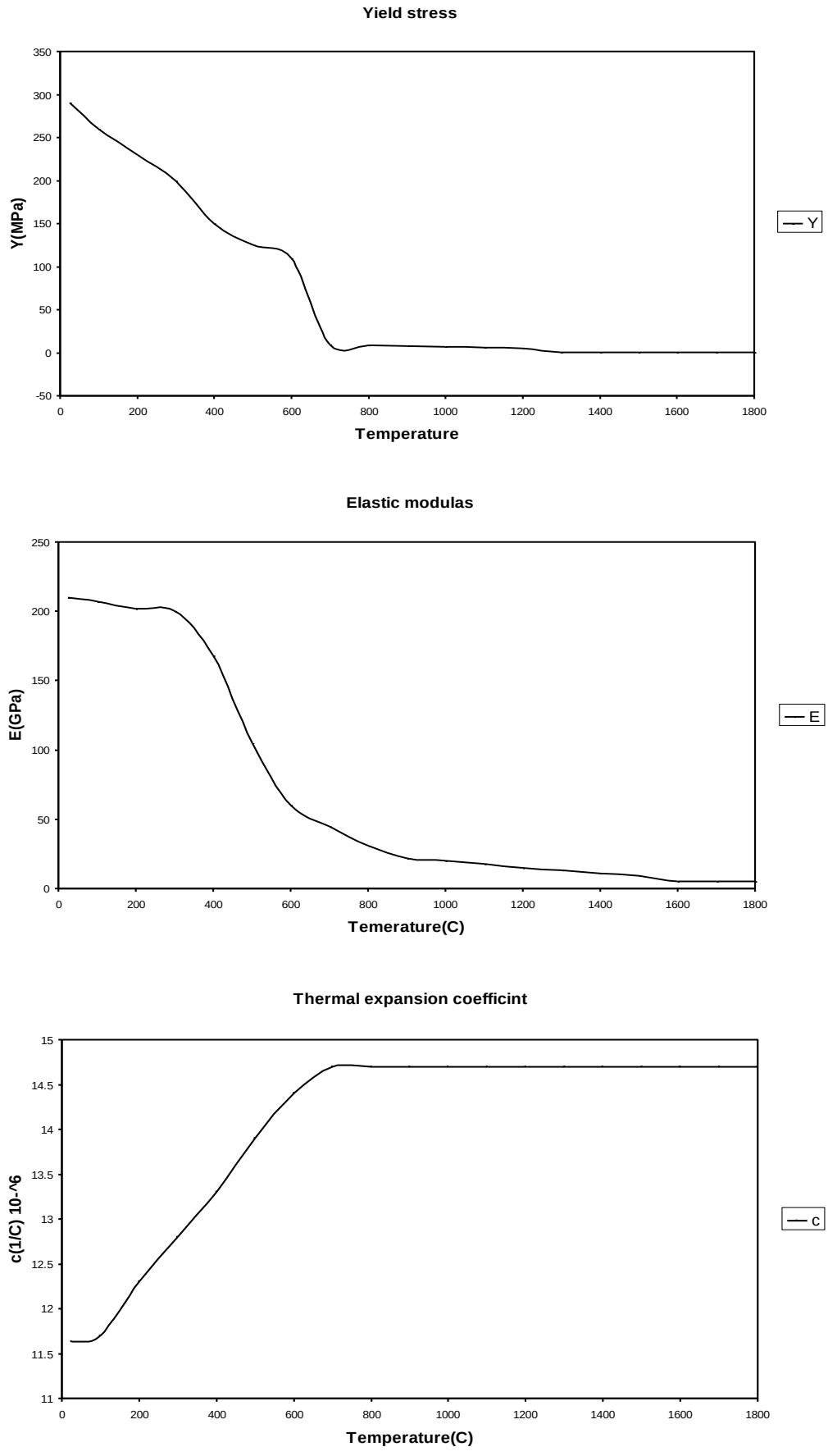

Fig. 7. Variation of Mechanical properties with temperature, Ajinomoto, 2001

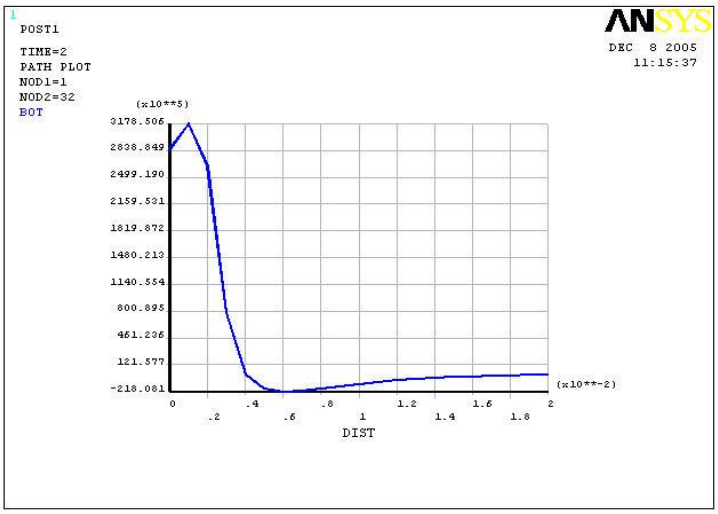

Fig. 8. Longitudinal Stress evaluated at middle Cross-Section – Bottom Surface through the Thickness

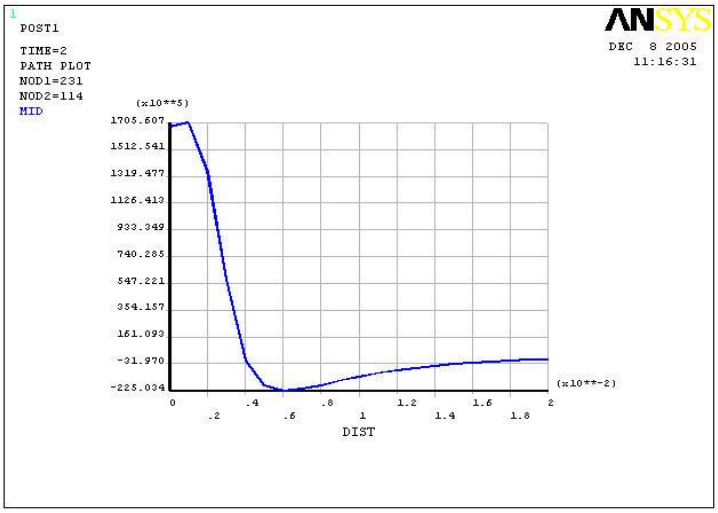

Fig. 9. Longitudinal Stress evaluated at middle Cross–Section – Mid Surface through the Thickness

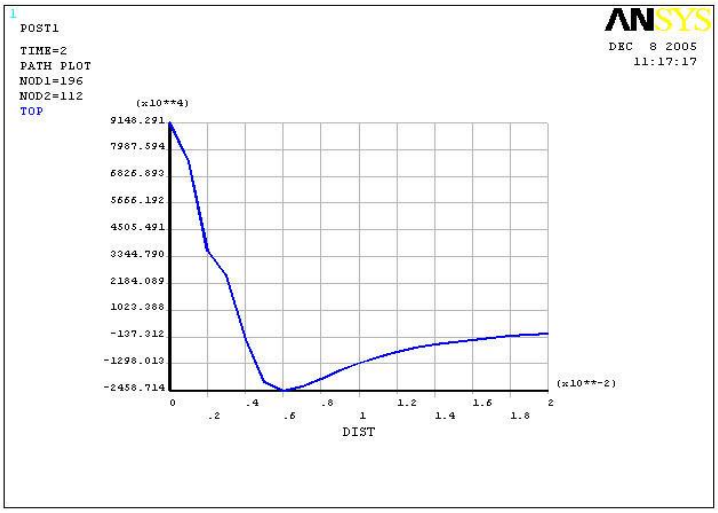

Fig. 10. Longitudinal Stress evaluated at middle Cross-Section – Top Surface through the Thickness

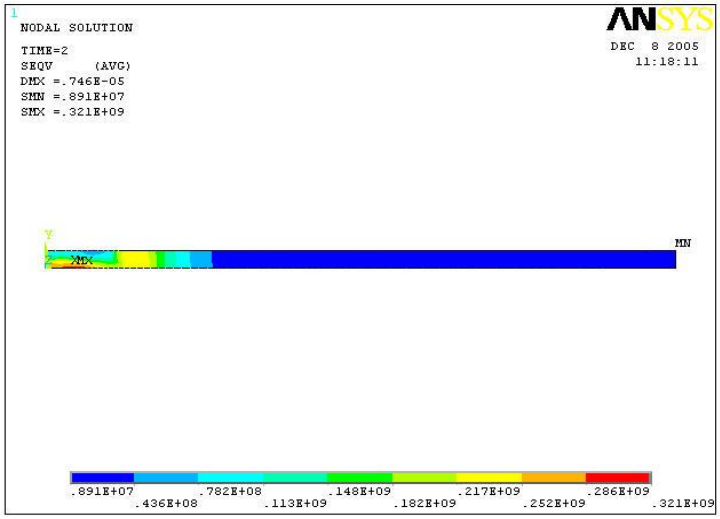

Fig. 11. Von Misses Stress Distribution

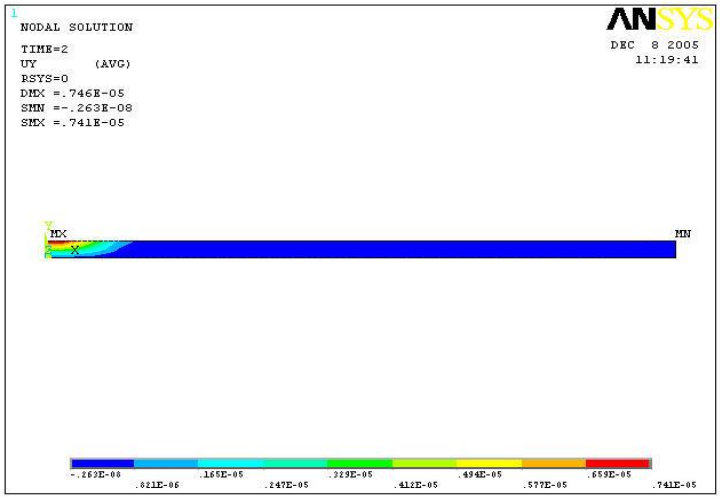

Fig. 12. Out – OF – Plane Displacement, UY

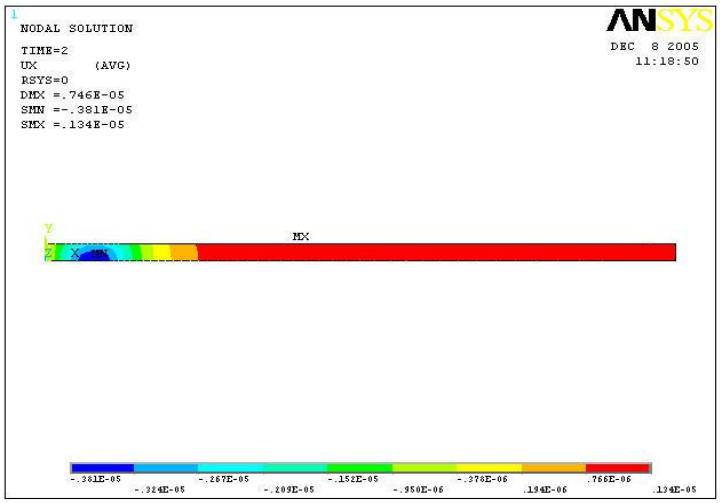

Fig. 13. UX Displacement